Coherent Structures and Entropy in Constrained, Modulationally Unstable, Nonintegrable Systems

Benno Rumpf and Alan C. Newell

Mathematics Institute, University of Warwick, Coventry CV4 7AL, United Kingdom

(Received 10 November 2000; published 13 July 2001)

Many studies have shown that nonintegrable systems with modulational instabilities constrained by more than one conservation law exhibit universal long time behavior involving large coherent structures in a sea of small fluctuations. We show how this behavior can be explained in detail by simple thermodynamic arguments.

DOI: 10.1103/PhysRevLett.87.054102 PACS numbers: 05.45.–a, 05.70.Ln, 47.27.–i

Many dynamical systems (e.g., self-focusing optical waves in Kerr-nonlinear media [1], Langmuir waves in a plasma [2], spurious large amplitude fluctuations which destroy numerical algorithms for partial differential equations (pde's) [3,4]) exhibit a type of universal behavior in which high peaks of some field emerge from a low amplitude noisy background. The formation of these coherent structures is radically different in integrable and nonintegrable systems. In the integrable systems such as the 1D nonlinear Schrödinger (NLS) equation [5], spatially periodic arrays of solitarylike pulses return periodically in time to their original states reflecting the regular phase space structure of nested tori. In the nonintegrable systems, these periodic arrays themselves undergo a second instability again of phase type, essentially due to a breakdown of Kolmogorov Arnold Moser tori. The subsequent Arnold diffusion corresponds to the fusing of solitary wave peaks [6,7]. The system eventually settles down to a stationary state characterized by robust coherent structures immersed in a sea of radiated wavelike fluctuations. In this Letter, we show that such states are the most likely solutions for systems with additional integrals corresponding to surviving symmetries, such as total particle number, angular momentum, or magnetization. Simple thermodynamic considerations explain that an increase of the entropy of the sea of wavelike fluctuations under these constraints requires the formation of coherent structures and give predictions which agree closely with the results of simulations. The observed behavior is common in a huge equivalence class of nonintegrable systems with constraints, and we use the Heisenberg spin chain [8] as a representative model. The Landau-Lifshitz equation,

$$\dot{\mathbf{S}}_n = \mathbf{S}_n \times [J(\mathbf{S}_{n-1} + \mathbf{S}_{n+1}) + S_{nz}\mathbf{e}_z], \qquad (1)$$

with Hamiltonian $H = \sum_n \frac{1}{2}(1 - S_{nz}^2) + J(1 - \mathbf{S}_n\mathbf{S}_{n+1})$ is a classical approximation of the dynamics of magnetic moments $\mathbf{S}_n = (S_{nx}, S_{ny}, S_{nz})$ on a set of lattice sites n. Large amplitude solutions are bounded since the vector $\mathbf{S}$ of the local magnetization is restricted to a sphere $|\mathbf{S}| = 1$. The lattice constant as a lower bound of possible wavelengths avoids leakage of energy to infinitesimally small space scales. The z axis is a symmetry axis of the Hamiltonian and therefore the total z magnetization $M_z = \sum_n S_{nz}$ is also conserved. The spin chain (1) may be regarded as an extension of the NLS equation, since, for ferromagnetic coupling $J > 0$, it can be approximated by the discrete focusing NLS-equation $i\dot{\phi}_n + J(\phi_{n+1} + \phi_{n-1} - 2\phi_n) + |\phi_n|^2\phi_n = 0$ in the limit of low-amplitude solutions. Both systems are nonintegrable even in one dimension and show very similar self-focusing behavior. In numerical simulations of a chain of 512 spins with periodic boundary conditions, we observe the self-focusing instability of the homogeneously magnetized state precessing about the z axis with the frequency $\omega = S_z$. A small perturbation leads in about 60 time units to a solution which, initially, is almost periodic in time and space. In Fig. 1, we plot the peaks (the sites where the spins differ most from the north pole) as a function of time. Figure 2 shows that initially ($t < 200$) energy is transferred periodically between the anisotropic $H_a = \sum_n \frac{1}{2}(1 - S_{nz}^2)$ and the coupling part

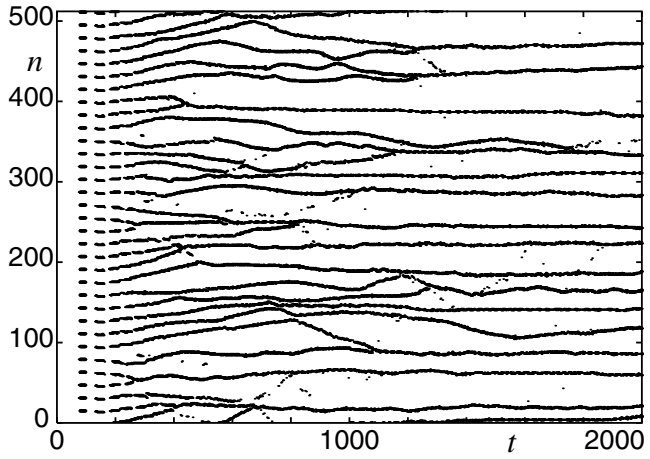

FIG. 1. Integration of 512 spins ($J = 0.4$) with periodic boundary conditions over 2000 time steps with a weakly perturbed homogeneous initial condition ($S_z \approx \sqrt{0.84}$). Lattice sites where the spins deviate significantly from the north pole ($S_z < 0.8$) are marked with dots. A similar pattern is obtained for the discrete focusing NLS.

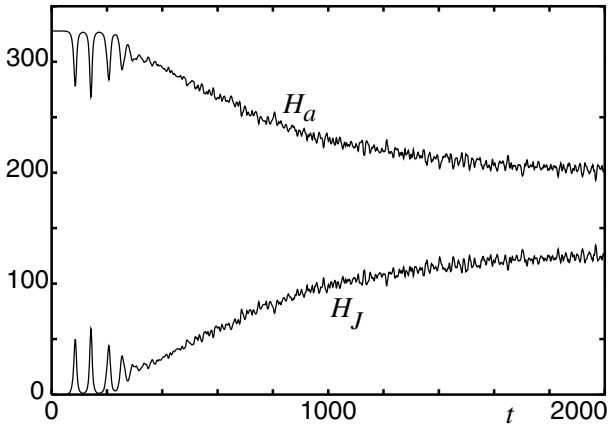

FIG. 2. Share of coupling energy and anisotropic energy over 2000 time steps.

$H_J = \sum_n J(1 - \mathbf{S}_n\mathbf{S}_{n+1})$ of the Hamiltonian. After another 150 time units, the second long wave phase instability [9–11] caused by the breakdown of periodic orbits of the almost periodic state is evident, and several peaks gradually move towards each other. After 250 time units, several of these peaks fuse and give rise to even larger ones whose spins deviate significantly from the north pole alignment. This Arnold diffusion phase (see Fig. 2, $250 < t < 1500$) coincides with an irreversible transfer of energy to the coupling part of the Hamiltonian and corresponds to an increase of high wave number fluctuations as the sea of spin waves near the north pole explores more and more of phase space. This process continues until the spins of some site domains are gathered close to the south pole leaving the other spins with small amplitudes near the north pole. Eventually, six xenocrysts of the south pole spins are pinned to the lattice and the energy transfer stops. Simulations through 200 000 time steps indicate a quasiequilibrium state with no further mergings on relevant time scales.

We describe the thermodynamic equilibrium resulting from this merging process by using a self-consistent approximation of the Hamiltonian. Since numerics indicates that eventually the spins deviate very little from the poles, the relevant part of the Hamiltonian in this state is a combination of coupled harmonic oscillators (S_{nx}, S_{ny}) and Ising spins $\sigma_n = \pm 1$,

$$\begin{aligned} H_{\text{eff}} &= H_w(S_{nx}, S_{ny}) + H_I(\sigma_n) \\ &= \sum_n \frac{1}{2}(S_{nx}^2 + S_{ny}^2) + J(S_{nx}^2 + S_{ny}^2) \\ &\quad - J(S_{nx}S_{n+1x} + S_{ny}S_{n+1y}) - J\sigma_n\sigma_{n+1}\,. \end{aligned} \quad (2)$$

Spins near the north or south pole are approximated as $S_{nz} \approx \sigma_n[1 - \frac{1}{2}(S_{nx}^2 + S_{ny}^2)]$. This approximation neglects the coupling of the oscillators $S_{nx/y}$ to the Ising spin σ_n by assuming that $\sigma_n\sigma_{n+1} = 1$ holds for almost all n; i.e., the domain walls contain little energy. In this limit, the magnetization, which is an exact second integral of motion, may be approximated as

$$\begin{aligned} M_{\text{eff}} &= M_I(\sigma_n) + M_w(S_{nx}, S_{ny}) \\ &= \sum_n \sigma_n - \frac{1}{2}(S_{nx}^2 + S_{ny}^2)\,, \end{aligned} \quad (3)$$

since we have observed that most of the spins point to the north pole. Again this approximation neglects higher order terms in $S_{x/y}$ and the fluctuations $\sigma_n S_{x/y}^2$ near the south pole $\sigma_n = -1$. Domains with $\sigma_n = -1$ represent the coherent structures. Our numerical study shows that the existence of the second integral of motion M is crucial for the fusion of peaks. Indeed, the fusions disappear and the spins remain near the north pole if the second integral of motion is destroyed by a symmetry breaking field. As a result, the statistical description requires the computation of the phase space surface on which M and H are constant. Using S_{nx} and S_{ny} as linear approximations of the canonical coordinates, the grandcanonical partition function for low energies may be computed as

$$\begin{aligned} Y(\beta, \gamma) &= \int e^{-\beta(H_{\text{eff}} - \gamma M_{\text{eff}})} d\Gamma \\ &= \left(\pi \frac{\cosh(\gamma\beta) + \mu}{A^2\beta}\right)^N, \end{aligned} \quad (4)$$

with the abbreviations $A = \sqrt{J/2 + [(1 + \gamma)/8]} + \sqrt{(1 + \gamma)/8}$ and $\mu = \sqrt{\sinh^2(\gamma\beta) + e^{-4J\beta}}$. In (4), β is the inverse temperature, γ is the equivalent of a magnetic field or a chemical potential, and $d\Gamma$ is the elemental phase space volume. The thermodynamic properties of the equilibrium state may be derived from the Gibbs potential $G(\beta, \gamma) = \beta^{-1}\ln(Y)$ when β and γ are calculated for M and H. The more appropriate thermodynamic potential is the entropy $S = \beta(H - G - \gamma M)$ written as a function of M and H. The old variables β, γ and the new variables H, M are connected by $M = \frac{1}{\beta}\frac{\partial}{\partial\gamma}\ln(Y)$, $H = (\frac{\gamma}{\beta}\frac{\partial}{\partial\gamma} - \frac{\partial}{\partial\beta})\ln(Y)$.

Since the truncation (2) of the Hamiltonian is valid for low energy excitations, we will discuss the entropy in the low temperature limit $\beta^{-1} \ll 1, \gamma \sim \beta^{-1/2}e^{-2J\beta} \ll 1$. The energy of the Ising magnet decreases exponentially as $H_I = 2JN\gamma^{-1}\beta^{-1}e^{-4J\beta} \sim \beta^{-1/2}e^{-2J\beta}$, and therefore it contains a very small number $H_I/(4J)$ of domain walls, but the number of spins that flip down may be proportional to $\sim\beta^{-1}$, the temperature. The spin waves provide the bulk of the energy $H \approx H_w$ and the entropy $S \approx S_w$. The entropy of the spin waves per lattice site turns out to be $S_w/N = \ln\Omega$, with the number of accessible microstates Ω per spin,

$$\Omega = [H_w + (4J + 1)M_w](H_w/M_w + 1)\,. \quad (5)$$

Figure 3 shows Ω, β^{-1}, and γ as a function of the magnetization of the spin waves. There are highly ordered

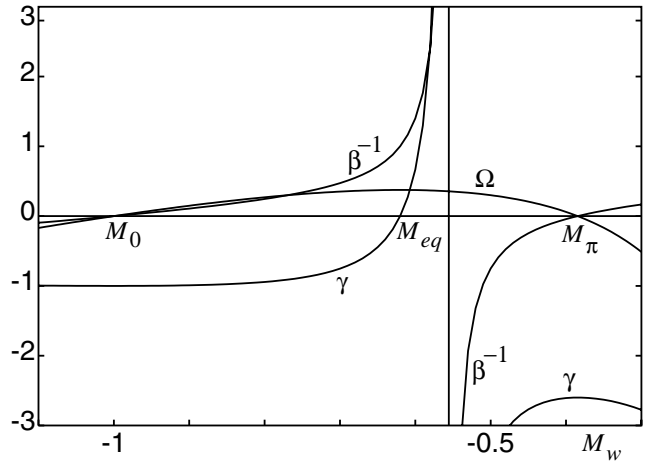

FIG. 3. Number of states Ω [Eq. (5)], temperature β^{-1} [Eq. (7)], and thermodynamic magnetic field (or chemical potential) γ of the spin wave system against the magnetization of the spin waves for $H_w = 1$, $J = 0.4$.

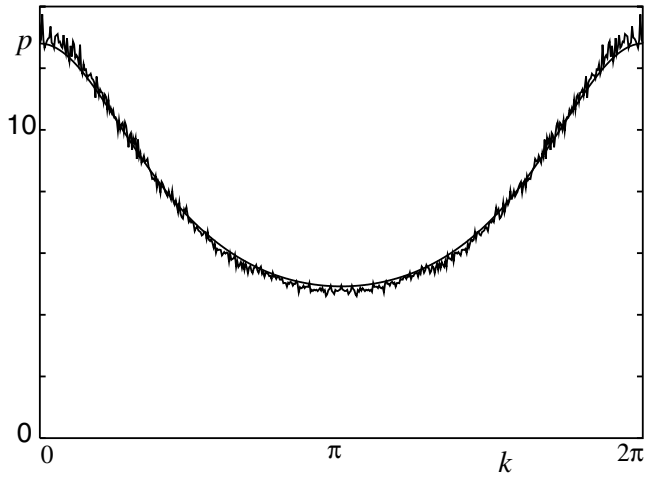

FIG. 4. Spatial power spectrum averaged over 100 000 time steps and the Rayleigh-Jeans distribution (6).

solutions $\Omega = 0$ for $M_w = M_0 \equiv -H_w$ and for $M_w = M_\pi \equiv -H_w/(4J + 1)$. These cases of maximal and minimal magnetization correspond to a spin wave with wave numbers 0 and π, respectively. $M_w = -H$ and $M_I = N$ corresponds to the initial condition of the simulation of Figs. 1 and 2. $M_0 \le M_w \le M_\pi$ defines the range of possible states with positive $\Omega(M_w)$; $\Omega(M_w)$ has a maximum at $M_{\rm eq} \equiv -H_w/\sqrt{4J + 1}$ for a given value of H_w where the Lagrange parameter $\gamma = -\frac{1}{\beta}\frac{\partial S}{\partial M_w}$ is zero. The spin waves with a wave number k contributes the power,

$$\langle n_k \rangle = \beta^{-1}[2J(1 - \cos k) + 1 + \gamma]^{-1}, \qquad (6)$$

to the Hamiltonian $H = \sum_k n_k \omega_k$, with $n_k = S_{kx}S_{-kx} + S_{ky}S_{-ky}$ and $\omega_k = 2J(1 - \cos k) + 1$. Our numerical work agrees perfectly with this Rayleigh-Jeans distribution $\langle n_k \rangle = T/(\gamma + \omega_k)$ (Fig. 4). The temperature of an equilibrium with a given magnetization M_w is

$$\beta^{-1} = \frac{(H + M_w)[H + (2 + 4J)M_w]}{2H + (1 + 4J)M_w}. \qquad (7)$$

The ordered states of a spin wave with $k = 0$ ($M_w = M_0$) or with $k = \pi$ ($M_w = M_\pi$) both correspond to zero temperatures. The state of maximal entropy has the temperature $\beta^{-1} = (1 + 4J)H/N$.

To maximize the entropy, the right amount of magnetization has to be allocated to the spin waves. This is possible because the Ising magnet can change its magnetization by flipping spins down or up. While the energy of the spin waves is fixed $H_w \approx H$, the magnetization $M_w = M - M_I < 0$ can be adjusted to the ideal value $M_{\rm eq}$ by turning over magnetization to the Ising part, $M_I = \sum \sigma_n$, when some of the spins flip down. The maximum entropy of the spin waves can be reached if the power is gathered on longer space scales initially so that the magnetization $M_w + M_I - N$ is smaller than $M_{\rm eq} = -H/\sqrt{4J + 1}$. The entropy generation is caused by the thermalization of the energy of this relatively ordered initial state. In this case, the system can increase M_w if it decreases M_I by flipping spins from the north to the south to keep $M_w + M_I$ constant. This is the statistical reason for the continuation of the focusing process: To increase the entropy of small-scale fluctuations, the system has to adjust their share of the second integral of motion. This is done by the formation of coherent pulses with high amplitudes. In Fig. 3 this means that the system is allowed to move from the left to the right to increase Ω in any case, but it may only move from the right to the left if the Ising magnetization is smaller than its maximum $M_I = N$. Figure 5 compares thermodynamical and numerical findings of the final ratio of anisotropic energy and coupling energy (corresponding to Fig. 2 after long integration times). The deviation for low coupling constants corresponds to a

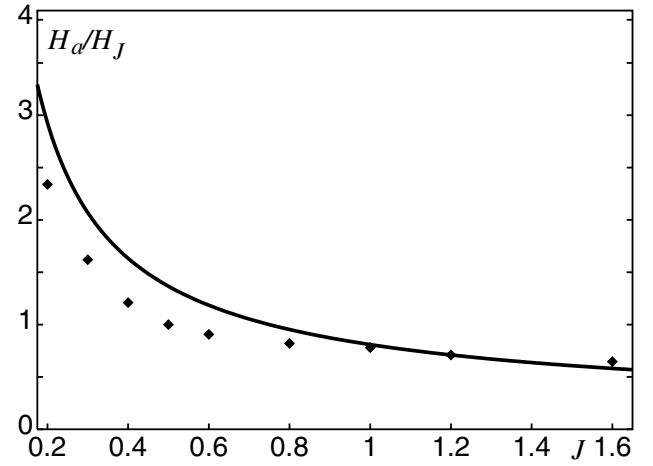

FIG. 5. Numerical (points) and thermodynamical (line) results for H_a/H_J against the coupling constant J after long integration times.

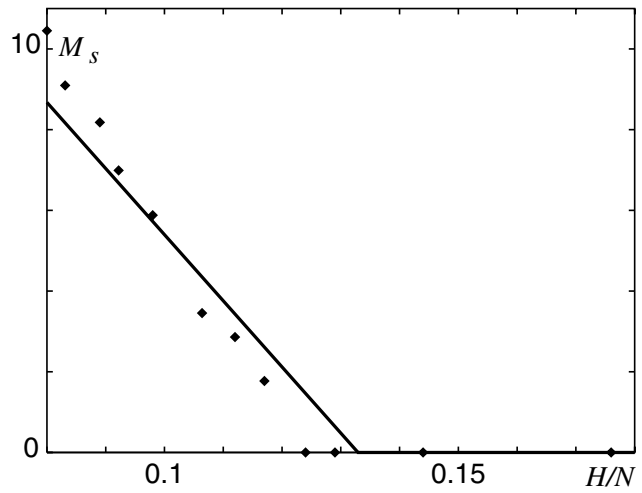

FIG. 6. Numerical (points) and results for the total magnetization $\sum_{n(S_{nz}<0)} |S_{nz}|$ of the spins in the southern hemisphere and thermodynamical prediction (line) for the share of spins that point down against the total energy per spin for $M/N = \sqrt{0.84}$.

surplus of domain walls that are still present after long integration times which do not exist in the thermodynamic equilibrium. The size of the coherent structures is given by the number of spins $M_S = (N - M_I)/2$ of the Ising magnet that point down. Figure 6 shows this number as a function of the energy per spin while the magnetization is fixed. For energies above the threshold $H = (N - M)\sqrt{4J + 1}$, only an exponentially small share of spins point down. For $M < N + M_{\text{eq}}$, the number of spins that condense at the south pole increases linearly as $M_S = (N - M - H/\sqrt{4J + 1})/2$. The curve in Fig. 6 is an analytic function, but it approaches a phase transition for decreasing temperatures. This emergence of coherent structures in the lowest order of the temperature is a consequence of the second integral of motion. The threshold does not occur in studies [12] of the thermodynamics of similar systems where the available phase space is not restricted by the second conserved quantity. The generation of an exponentially small number of strongly nonlinear structures in these systems is a purely thermal effect.

The phenomenon we have described is widespread. One of us (A. C. N.) encountered it in numerical algorithms for pde's. In [3,4] it was shown that, despite a choice of algorithms designed to remove all fast instabilities, nonintegrable focusing eventually produces local errors large enough to overcome nonlinear instability thresholds. It was also seen by Dyachenko *et al.* [6] in a near integrable extension of the NLS equation which is the small amplitude continuum limit of (1). In a soliton collision, they found that the stronger one becomes stronger and the weaker one becomes weaker. Radiation which enhances the entropy of the wave field is produced. In order that the independent Hamiltonian $H = \int (|\nabla\phi|^2 - |\phi|^4)\, dV$ and particle number $N = \int |\phi|^2\, dV$ are conserved, an increase in $\int |\nabla\phi|^2\, dV$ must be accompanied by an increase in peaks with high $|\phi|$ values.

The physical conclusion of this result is that the continuing focusing process is driven by the generation of entropy in a state of small amplitude waves. The link between the entropy and the emergence of peaks is the constraint by two integrals of motion. In terms of equation (6), an initial distribution of particles n_k will not be able to reach the Rayleigh-Jeans distribution while obeying both the conservation of energy $\sum n_k \omega_k$ and the particle number $\sum n_k$. But the restriction of particle conservation may be circumvented by gathering low-energy particles in small domains and transferring energy to the remaining particles to increase the overall entropy. The peaks created by the self-focusing process are therefore condensates of low-energy particles. In that sense, the formation of peaks has a formal similarity to the condensation of droplets in oversaturated steam where the entropy is maximized under the restriction of particle conservation.

B. R. gratefully acknowledges support by a grant of German Academic Exchange Service (DAAD). A. C. N. gratefully acknowledges support from NSF Grant No. DMS 0072803.

[1] P. L. Kelley, Phys. Rev. Lett. **15**, 1005 (1965); A. J. Canpillo, S. L. Shapiro, and B. R. Suydam, Appl. Phys. Lett. **23**, 628 (1973).
[2] V. E. Zakharov, Zh. Eksp. Teor. Fiz. **62**, 1743 (1972) [Sov. Phys. JETP **35**, 908 (1972)].
[3] A. C. Newell, SIAM J. Appl. Math. **33**, 1 (1977).
[4] W. Briggs, A. C. Newell, and T. Sarie, J. Comput. Phys. **51**, 83 (1983).
[5] V. E. Zakharov and A. B. Shabat, Zh. Eksp. Teor. Fiz. **61**, 118 (1971) [Sov. Phys. JETP **34**, 62 (1972)].
[6] A. I. Dyachenko, V. E. Zakharov, A. N. Pushkarev, V. F. Shvets, and V. V. Yankov, Zh. Eksp. Teor. Fiz. **96**, 2026 (1989) [Sov. Phys. JETP **69**, 1144 (1989)].
[7] S. Dyachenko, A. C. Newell, A. Pushkarev, and V. E. Zakharov, Physica (Amsterdam) **57D**, 96 (1992).
[8] A. M. Kosevich, B. A. Ivanov, and A. S. Kovalev, Phys. Rep. **194**, 117 (1990); B. Rumpf and H. Sauermann, Phys. Rev. E **58**, 1463 (1998).
[9] M. J. Ablowitz and B. M. Herbst, SIAM J. Appl. Math. **50**, 339 (1990).
[10] D. W. McLaughlin and C. M. Schober, Physica (Amsterdam) **57D**, 447 (1992).
[11] A. Calini, N. M. Ercolani, D. W. McLaughlin, and C. M. Schober, Physica (Amsterdam) **89D**, 227 (1996).
[12] J. A. Krumhansl and J. R. Schrieffer, Phys. Rev. B **11**, 3535 (1975); K. Nakamura and T. Sasada, J. Phys. C **11**, 331 (1978); J. Villain, in *Ordering in Strongly Fluctuating Condensed Matter Systems,* edited by T. Riste (Plenum Press, New York, 1980), p. 91.